Correlations and structure factor of bicontinuous microemulsions

S. T. Milner ([1]), S. A. Safran ([1]), D. Andelman ([1,*]), M. E. Cates ([2,**]) and D. Roux ([3])

([1]) Corporate Research Science Laboratories, Exxon Research and Engineering Company, Annandale, NJ 08801, U.S.A.
([2]) Institute for Theoretical Physics, University of California, Santa Barbara, CA 93106, U.S.A.
([3]) Centre de Recherche Paul Pascal, Domaine Universitaire, 33405 Talence Cedex, France

Résumé. — On calcule des fonctions de corrélation et le facteur de structure de microémulsions par une approche de thermodynamique statistique ; cette approche avait été utilisée auparavant pour obtenir les diagrammes d'équilibre des phases. Le facteur de structure $S(\mathbf{q})$ a un pic pour un vecteur d'onde $q_{max} \approx \pi/\xi$ où ξ est la taille des domaines d'huile et d'eau. L'origine physique de ce pic est liée aux corrélations introduites par l'énergie de courbure du film tensioactif ; la renormalisation du module de courbure par les fluctuations thermiques joue un rôle important dans la stabilité de ces fluctuations. En représentant ces corrélations dans l'espace réel, on montre qu'il y a plusieurs types de corrélations, de vecteurs **q** différents, qui contribuent de manière importante à $S(\mathbf{q})$.

Abstract. — The correlation functions and structure factor of microemulsions are calculated from a statistical thermodynamic approach which has been previously used to obtain the equilibrium phase diagrams. The structure factor, $S(\mathbf{q})$, has a peak at a wavevector $q_{max} \approx \pi/\xi$ where ξ is the domain size of the oil and water regions. The physical origin of this peak are the correlations induced by the presence of the curvature energy of the surfactant film ; the renormalization of the bending modulus by thermal fluctuations plays an important role in stabilizing these fluctuations. Real space representations of these correlations show that there is significant strength in $S(\mathbf{q})$ from several different wavevectors.

1. Introduction.

Microemulsions are three-component solutions of water, oil, and surfactant where the oil and water have separated into domains with length scales on the order of tens to hundreds of Angstroms, with a surfactant monolayer at the internal water/oil interface [1]. Some systems form globular domains [2] while others are composed of bicontinuous [3] regions of water and oil with no particular globular structure. These changes in structure (and associated properties such as phase behaviour, interfacial tensions, diffusivity, etc.) can be affected by changing the surfactant, temperature or salinity, or adding cosurfactant. Theoretically, the evolution of the microemulsion structure from globules of water in oil, to a bicontinuous structure, to globules of oil in

water, can be understood in terms of a change in the *spontaneous radius of curvature* of the surfactant film [4-8]. The bicontinuous structure occurs when the volume fractions of water and oil are comparable, and the surfactant interface is chemically balanced so that there is no spontaneous curvature towards either the oil or the water.

The theoretical understanding of the bicontinuous phase has focused on the multi-phase equilibria observed experimentally, and on the transition between the isotropic microemulsion and on ordered lamellar phase [4, 6, 9, 10, 11]. In these treatments, the structure of the microemulsion is considered at the level of random mixing of the water and oil domains (often represented on a coarse-grained lattice) with no correlations between the regions. Other approaches [12-15] have focused on *microscopic* lattice models for microemulsions. These approaches, however, have not yet been developed to the level of predicting the large length scale, bicontinuous structures seen in these systems.

(*) *Present address :* School of Physics and Astronomy, Tel-Aviv University, Ramat-Aviv 69978, Israel.
(**) *Address from January 1, 1988 :* Cavendish Laboratory, Madingley Road, Cambridge CB3 OHE, G.B.

Recently, there have been several experimental studies of the structure of bicontinuous microemulsions [16-20]. Globular microemulsions have been extensively studied in the past [2] ; scattering from such systems can often be interpreted in terms of interacting hard sphere models, although some non-spherical systems may also exist [21-23]. The structural studies of bicontinuous microemulsions have consisted of light, neutron, and X-ray scattering as well as freeze-fracture microscopy [24]. The scattering structure factor of the bicontinuous systems (or, more specifically, middle-phase microemulsions which coexist with both oil and water) show the following features for a wide variety of systems [16-20] :

(i) scattering at large wavevectors **q** which obeys a Porod law (intensity proportional to q^{-4}) with corrections due to the finite thickness of the interface. The Porod law breaks down at a characteristic length scale related to the curvature of the interface [16] ;

(ii) a peak in the intensity at smaller values of $q = q_{max}$ with a half-width of the order of q_{max} ;

(iii) the ratio of the characteristic size obtained from q_{max} to that obtained from the breakdown of the Porod law is about 2 [16].

In this paper, we present an extension of our thermodynamic model for microemulsions to calculate the correlation functions and structure factor of balanced systems. Our calculations result in a structure factor with a peak at $q_{max} \cong \pi/\xi$, where ξ is the domain size of the water and oil regions. The physical origin of this peak are the correlations induced by the presence of the curvature energy [25]. (In any lattice model, scattering from even randomly positioned water and oil domains results in Bragg peaks in the structure factor at $q_0 = 2 \pi/\xi$, corresponding to the reciprocal lattice vector. We regard our lattice model as an approximate means of representing microemulsions which includes a domain size ξ and may be used to investigate local correlations in the position of oil and water domains ; we regard as spurious the Bragg peaks which arise from the long-range order of the centers of distant domains.)

Previous theoretical treatments of the structure and scattering from bicontinuous phases have been of two sorts : (i) extensions of thermodynamic models, such as that of Talmon and Prager [26], which fail to predict a peak in the scattering due to the lack of correlations in the model ; (ii) geometrical theories for the structure factor which rely on either an assumed form for the scattering [17, 18] or a highly constrained microstructure [19]. Although they fit the experimental data reasonably well, these latter calculations have no thermodynamic origin ;

the $q \to 0$ limit of these theories does not originate from a free energy which is capable of predicting the equilibrium phase diagram. In contrast, the present work extends our treatment [7, 8] of the thermodynamics to include fluctuations ; the same theory predicts the phase diagram, the scattering peak, and the microstructure.

The organization of this paper is as follows : section 2 reviews the microemulsion model and its extension to treat spatial correlations. Our results for both the structure factor and a consistent microstructure are presented in section 3. In section 4, we summarize our results and conclusions.

2. Microemulsion model.

In the present work, we consider *balanced* microemulsions with no spontaneous curvature. (Extensions of the thermodynamic model to systems with spontaneous curvature have been treated in Refs. [7, 8, 27]). In the balanced case it is observed that for equal water and oil volume fractions, the system is liquid and isotropic (bicontinuous microemulsion) at small values of the surfactant volume fraction ϕ_s. For large values of ϕ_s, there is a transition to a lamellar phase, while for values of ϕ_s smaller than some minimum value there is a multi-phase region in the phase diagram, as shown in figure 1. De Gennes and Taupin [4] suggested that the microemulsion phase is only stable when the surfactant film separating the water and oil regions is not too stiff ; otherwise the structure is lamellar, since the bends induced in the surfactant monolayer by the isotropy of the microemulsion are energetically too costly.
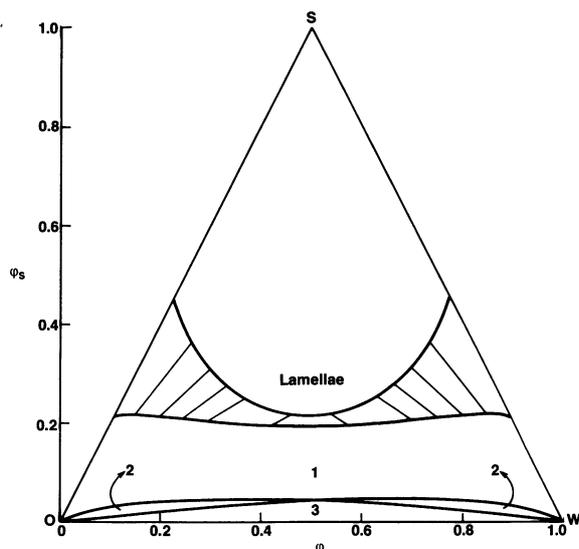

Fig. 1. — Calculated phase diagram for microemulsions from reference [8]. The numbers represent the number of coexisting phases in the multiphase region, with 1 representing the single-phase, random micromulsion. (The figure shown is for $\pi K/T = 1.25$, $\alpha = 1$.)

For films that are not too stiff, the microemulsion phase is more stable than the lamellar phase due to the increased entropy of the surfactant interface. This entropy was first estimated by Talmon and Prager [10] who considered the entropy of mixing of the water and oil regions.

Recently, we have presented [7, 8] a thermodynamic model for microemulsions which takes into account not only the entropy of the interface but also its bending energy. Our model results in a phase diagram which is in qualitative agreement with experiment (see Fig. 1) and includes the multi-phase region as well as the transition to the lamellar phase. This model is distinct from those of references [4, 6] in its treatment of the thermal fluctuations of the surfactant interface *via* a length scale dependent bending constant [28-30].

Following references [7, 8], we consider a lattice with unit cell size ξ, each cell filled with either oil or water, with the surfactant at the oil/water interface. The domain size ξ is determined by the constraint that the interfacial surfactant film is an incompressible two-dimensional fluid. In a random mixing approximation where $\xi \equiv \xi_{rm}$, this implies that

$$\xi_{rm} = az\phi (1 - \phi)/\phi_s . \tag{1}$$

Here z is the coordination number of the lattice (which we will take to be cubic, thus $z = 6$); $\phi - \phi_s/2$ and $(1 - \phi) - \phi_s/2$ are the water and oil volume fractions; ϕ_s is the surfactant volume fraction; and a is a microscopic length. (The main effect of choosing some other lattice, and hence some other value of z, is to alter the numerical value of ξ for given ϕ and ϕ_s, which is equivalent to changing the value of a.) By introducing a length scale dependent bending modulus [28-30], $K(\xi)$, for the surfactant film, we find that the single phase microemulsion is only stable when it structural length scale ξ is of order ξ_K, the persistence length of the film. The persistence length is related to the bare bending constant K_0 ($K_0 = K(a)$, with a being a molecular size) by the relation [4]

$$\xi_K = \exp (4 \pi K_0/aT)$$

where α is a constant of order unity whose value is discussed below. For length scales $\xi \approx \xi_K$, the effective bending modulus is of order T. At large values of ϕ_s, $\xi \ll \xi_K$ and $K(\xi) \gg T$; the lamellar phase is stable. At small values of ϕ_s, a multiphase region occurs due to the presence of an inflection point in the free energy for values of ϕ_s corresponding to ξ of order ξ_K in equation (1) [8].

In the present work, we extend this model to study correlations in the microemulsion. As before, we consider an incompressible surfactant film bounding the internal water/oil regions, which are arranged on a lattice of size ξ. This condition which conserves the total amount of surfactant can be written for an arbitrary configuration of water and oil domains :

$$\xi = \frac{1}{N} \sum_{ij} J_{ij} s_i (1 - s_j)/\phi_s \tag{2}$$

where $s_i = 0,1$ indicates that cell i is filled with oil or water respectively. The tensor J_{ij} equals one for nearest neighbour cells i and j, and is zero otherwise. In the random mixing approximation, this reduces to the relation (1) between ξ_{rm} and ϕ_s stated above.

We note that in equation (2), the sums on i and j run over the N cells of the lattice. However, for fixed total volume V, $N = V/\xi^3$. Thus, N depends on the configurations *via* equation (2). This has no effect on equation (2) itself since ξ is an intensive variable and has a value that is independent of N as long as N is large. Extensive quantities such as the thermodynamic potential, G, will have an added dependence on the configurations because of the relation between N and ξ. We take this into account by writing the thermodynamic potential, G, as

$$G = \frac{V}{\xi^3} f - \Lambda M \tag{3}$$

where f is the free energy per site, Λ is a Lagrange multiplier which fixes the average value of the water and oil volume fractions, and $M = \frac{1}{N} \sum_i s_i$.

The structure factor can be calculated as the Fourier transform of the correlation function χ_{ij}, where

$$\chi_{ij} = \langle s_i s_j \rangle - \langle s_i \rangle \langle s_j \rangle . \tag{4a}$$

The angle brackets denote a thermal average. In order to calculate χ_{ij}, we introduce a set of local fields, h_i, into the Hamiltonian, H, so that

$$H = H_b - \sum_i h_i s_i \tag{4b}$$

where H_b is the bending Hamiltonian. The correlation function is calculated from the thermodynamic potential G, as

$$\chi_{ij} = \frac{1}{\beta} \frac{\partial^2 G}{\partial h_i \partial h_j} = - \frac{\partial m_i}{\partial h_j} \tag{5}$$

where $m_i \equiv \langle s_i \rangle$, and all the derivatives are evaluated at $\{h_i\} = 0$. The potential G is calculated from the partition function in the usual manner, while the partition function is calculated within a single-site approximation as detailed below.

Following reference [8], we now consider the bending energy H_b for the surfactant film located at the water/oil interface. Strictly speaking, for a lattice model, the bends occur at the cube edges. However, we estimate the bending energy by rounding out

these edges to form sections of spheres of radius $\xi/2$. In addition, in the interest of simplicity, we neglect the saddle-splay contribution to the bending energy.

To obtain H_b for an arbitrary configuration of water and oil domains, we consider the arrangement of cell edges depicted in figure 2. All other arrangements carry no bending energy. In terms of the local cell occupancies $\{s_i\}$ on a cubic lattice, the bending Hamiltonian for the case of no spontaneous curvature is then :

$$H_b = (2\,\pi K(\xi)/3)\Big(\sum_{ij} (-4\,\mathbf{J}_{ij}\,s_i\,s_j +$$

$$+ \mathbf{J}_{ij}\,s_i\,s_j + 2\,\mathbf{J}_{ij}\,s_i)$$

$$+ \frac{1}{8}\,(C-4)\sum_{ijkl} \mathbf{M}_{ijkl} \times$$

$$\times \{s_i(1-s_j)(1-s_k)\,s_l +$$

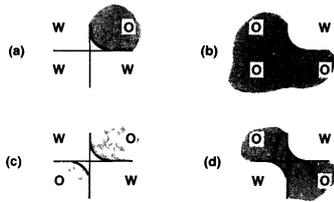$$+ (1-s_i)\,s_j\,s_k(1-s_l)\}\,\Big).\qquad(6a)$$

Fig. 2. — Four types of neighbouring edge configurations in a microemulsion. The letters O and W represent oil and water regions respectively. The radius of the bends is of order ξ.

The coupling tensor $\mathbf{L}_{ij}$ is equal to one if cells i and j are next nearest neighbours (i.e., have a common edge but no common face) and is equal to zero otherwise, while $\mathbf{M}_{ijkl}$ is equal to one if cells i, j, k, and l form the corners of an elementary plaquet with the pairs (i, l) and (j, k) being next nearest neighbours. Otherwise, $\mathbf{M}_{ijkl}$ is zero. In equation (6a), $K(\xi)$ is the length scale dependent bending constant discussed above and in references [28-30], while C is a parameter introduced here which accounts for the energy of the diagonal configurations shown in figures 2c and 2d. The random mixing approximation used in references [6-10] considers only triplets of cells which share an edge, and is equivalent to choosing a value of $C = 4$ and setting each $s_i = \phi$. This results in the vanishing of the quartic terms in equation (6a) and reduces to the random mixing form of the bending energy used in references [7, 8]

$$H_{b_{rm}} = 8\,\pi K(\xi)\,N\phi\,(1-\phi)\,.\qquad(6b)$$

It may be argued that a more realistic choice may be

to choose $C = 2$, which would correspond to assigning two bends to the configurations shown in figures 2c and 2d. (The random mixing approximation effectively assigns four bends to these diagonal arrangements.) Values of $C < 2$ may correspond to attractive interaction between adjacent pieces of interface, while values of $C > 2$ may correspond to an effective repulsive interaction. Such a repulsion could arise, for example, from steric hindrance of the fluctuating interfaces or from electrostatic interactions. In any case, we present our results as a function of C and $K(\xi)$.

The potential G is calculated from the Hamiltonian in a single-site approximation, including the inhomogeneous fields $\{h_i\}$. This method is equivalent to an expansion in small departures from random mixing, as may be checked rather laboriously by expanding directly, taking care to allow for the dependence of ξ on $\{s_i\}$ of equation (2). We assume the most general single-site statistical weight $P[\{s_i\}]$ given by [31]

$$P[\{s_i\}] \propto \prod_i e^{-\gamma_i s_i}\qquad(7)$$

and minimize the thermodynamic potential with respect to the set of parameters $\{\gamma_i\}$. An upper bound on the exact potential G of the system is given by

$$G = -TS_0 + \langle H\rangle_0 - \Lambda\langle M\rangle_0\qquad(8)$$

where $S_0 = -\mathrm{Tr}\,(P \log P)$ is the entropy of the trial statistical weight (Eq. (7)) and $\langle\,.\,\rangle_0$ signifies the expectation value using this weight. To get a least upper bound on the free energy, we minimize G with respect to $\{\gamma_i\}$. This determines the local order parameters $\{m_i\}$, given by the minimum over the $\{\gamma_i\}$ of the sum over configurations $m_i = \sum s_i\,P[\{s_i\}]$, as a function of the local fields $\{h_i\}$. Finally, we find the correlation function from equation (5) by taking field derivative of the $\{m_i\}$.

The results of this procedure are now described. The free energy per site f of equations (3) and (8) is found using the statistical weight of equation (6) :

$$f = \frac{1}{N}\Big[\sum_i T[(m_i \log (m_i)) +$$

$$+ (1-m_i)\log (1-m_i)]$$

$$+ H_b(\{m_i\}) - \sum_i h_i\,m_i\Big].\qquad(9)$$

In the random mixing approximation [7, 8], the free energy is

$$f_{rm} = T[\phi \log \phi + (1-\phi)\log (1-\phi)] +$$

$$+ 8\,\pi K(\xi)\,\phi\,(1-\phi)\,.$$

For the general case of equation (9) $\{m_i\}$ are the expectation values of the occupancies $\{s_i\}$ and are given by

$$m_i = (1 + e^{\gamma_i})^{-1}.$$

In equation (9), $H_b(\{m_i\})$ is obtained from equation (6) by setting $s_i \to m_i$. As noted above, f is independent of N in the limit of large N; the dependence of N on ξ and hence on the $\{m_i\}$ enters only via equation (3). We minimize G of equation (2) with respect to the $\{m_i\}$, which is equivalent to minimizing with respect to the $\{\gamma_i\}$. In the absence of the inhomogeneous fields, $m_i = \langle s_i \rangle = \phi$, and equation (9) reduces to a random mixing approximation. In the presence of the $\{h_i\}$, we find

$$\frac{\partial f}{\partial m_i} + \frac{\partial \xi}{\partial m_i} \left[-\frac{3}{\xi}\frac{f}{} + \frac{\partial K}{\partial \xi} \frac{H_b(\{m_i\})}{NK(\xi)} \right] = \frac{\Lambda}{N} \quad (10)$$

with $\xi = \xi(\{m_i\})$ given by

$$\xi(\{m_i\}) = \frac{a}{\phi_s} \frac{1}{N} \sum_{ij} J_{ij} m_i(1 - m_j). \quad (11)$$

The form of $K(\xi)$ has been discussed in references [28-30]. In the absence of more definitive calculations, we use the perturbation theory form :

$$K(\xi) = K_0 \left(1 - \alpha \frac{T}{4\pi K_0} \log(\xi/a) \right) \quad (12)$$

where a is a microscopic length, K_0 is the bare bending constant and the value of α is discussed below. Differentiating equation (10) with respect to the fields [32] as in equation (5) and setting the $\{h_i\} = 0$, we find an equation for the correlation function, χ_{ij} :

$$\frac{T}{N} \chi_{ij}^{-1} = \frac{\partial^2 f}{\partial m_i \, \partial m_j} +$$
$$+ \left[-\frac{3}{\xi}\frac{f}{} + \frac{\partial K}{\partial \xi} \frac{H_b(\phi)}{NK(\xi)} \right] \frac{\partial^2 \xi}{\partial m_i \, \partial m_j}. \quad (13)$$

The structure factor is the Fourier transform of the correlation function χ_{ij}, which is determined by equations (9), (11), (13) evaluated with $\{h_i\} = 0$ (and thus $\{m_i\} = \phi$). The result is [33]

$$S(\mathbf{q}) \equiv N^{-1} \sum_j e^{i\mathbf{q}\cdot(R_i - R_j)} \chi_{ij} \quad (14)$$

$$= \phi(1 - \phi)[1 + \varepsilon(\cos q_x\, \xi + \cos q_y\, \xi +$$
$$+ \cos q_z\, \xi) + \delta(\cos q_x\, \xi \cos q_y\, \xi$$
$$+ \cos q_y\, \xi \cos q_z\, \xi + \cos q_x\, \xi \cos q_z\, \xi)]^{-1}. \quad (15)$$

The quantities ε and δ are functions of C, the bending constant $K(\xi)$ (with ξ given by equation

(1), the random mixing expression), and the volume fractions :

$$\varepsilon = \frac{16\,\pi K(\xi)}{3\,T}\,\phi(1 - \phi) \times$$
$$\times [1 - (C - 4)\,\phi(1 - \phi)/2]$$
$$+ 2[\phi \log(\phi) + (1 - \phi)\log(1 - \phi)]$$
$$+ \frac{4\,a}{3}\,\phi(1 - \phi)[1 - (C - 4)\,\phi(1 - \phi)/2]$$
$$\qquad\qquad\qquad\qquad\qquad (16)$$

$$\delta = \frac{8\,\pi K(\xi)}{3\,T}\,\phi(1 - \phi)[(C - 4) +$$
$$+ 2 - 2(C - 4)\,\phi(1 - \phi)]. \quad (17)$$

The terms included in ε represent the effects of all nearest neighbour interactions, while those included in δ are all from next nearest neighbours. The unusually complicated forms of ε and δ are due in part to the quartic terms in the bending energy. More fundamentally, they arise from the dependence of the *lattice constant*, $\xi(\{m_i\})$, on the configurations of the system. This represents a basic difference between our model of the random microemulsion and related Ising models where the lattice constant is independent of the state of the system. As we shall see below, this unusual feature of the physics of the microemulsion is responsible for instabilities that are not present in the simple Ising systems.

3. Interpreting the calculated $S(\mathbf{q})$.

The structure factor calculated in the previous section depends on four parameters : $K(\xi)/T$, ϕ, α, and C. Not all values of these parameters correspond to physically realizable microemulsions. We need consider only the parameters for which : (i) $S(\mathbf{q})$ is finite and (ii) the microemulsion is more stable than competing phases (e.g., lamellae, or a two-phase coexistence of oil-rich and water-rich phases).

In section 3.1, the region of parameter space for which the calculated $S(\mathbf{q})$ is finite (so that the microemulsion is linearly stable against fluctuations) is examined, and the instabilities at the boundaries of this region are investigated. The first-order phase boundaries which separate the microemulsion from lamellae and from coexisting oil-rich and water-rich phases are then estimated.

In section 3.2, we discuss the calculated and observed structure factors. $S(\mathbf{q})$ is examined within the region of parameter space where conditions (i) and (ii) above hold, so that the microemulsion is both linearly and globally stable. There we find that the correlations present in the model are small ; thus the calculation of section 2, which expands about random mixing to lowest order in the correlations, is self-consistent. The artifacts introduced by the lattice in the model are examined, the dependence of

$S(\mathbf{q})$ on the restricted range of parameters is described, and the nature of the correlations in real space is discussed.

3.1 INSTABILITIES OF $S(\mathbf{q})$. — It can be shown that the divergences or instabilities of $S(\mathbf{q})$ (as a function of the parameters ε and δ of Eq. (15)) first appear at either $\mathbf{q} = 0$, corresponding to phase-separation of oil and water, or at one of the *antiferromagnetic* orderings [33] of near neighbours ($\mathbf{q} = (\pi/\xi, 0, 0)$, i.e. (100)), second neighbours ($\mathbf{q} = (\pi/\xi, \pi/\xi, 0)$, i.e. (110)), or third neighbours ($\mathbf{q} = (\pi/\xi, \pi/\xi, \pi/\xi)$, i.e. (111)). (These orderings are illustrated in Fig. 3). The region of parameters C and K/T over which $S(\mathbf{q})$ is finite and positive (i.e., the region of linear stability) is shown in figure 4 (for $\alpha = 0$, or no bending constant renormalization) and figure 5 (with $\alpha = 3$, a value chosen to enhance the effect of the renormalization).
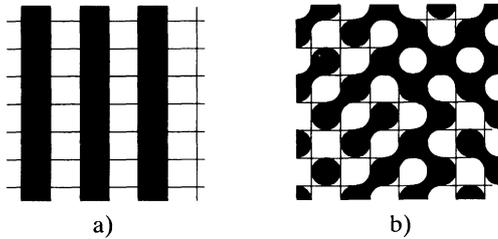

a)   b)

Fig. 3. — The simple cubic lattice permits several relevant morphologies to be represented. Lamellar order (planes normal to the page), corresponding to $\mathbf{q} = (100)$, is shown in figure 3a. *Tubular* order (tubes normal to the plane), corresponding to $\mathbf{q} = (110)$, is shown in figure 3b. The *double bends* in figure 3b are degenerate and have been assigned at random between the two possible diagonal configurations. A slice of cubic bicontinuous ordering with $\mathbf{q} = (111)$ looks the same as figure 3b ; however, the (110) case has ferromagnetic ordering in the third direction, while the (111) case is antiferromagnetic in the third direction such that black and white are reversed in the next layer.

3.1.1 Antiferromagnetic instabilities. — The present calculation of $S(\mathbf{q})$ goes beyond random mixing to include fluctuations in the arrangement of the oil and water regions. In addition, we necessarily include the effects of concentration fluctuations on the average lattice size ξ as well, because of equation (2). For a single phase in a constant-volume system, specifying the volume fraction ϕ_s determines the amount of interface in the system. In fact, equation (2) tells us that $\phi_s \xi/a$ is equal to the average number of interfaces (squares separating oil and water) per cell. This means that the average lattice size in our model depends on the configuration being considered. (We are not including local fluctuations in the domain size ξ, which are difficult
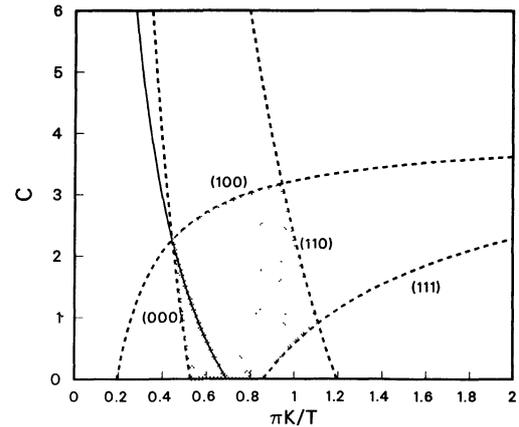

Fig. 4. — Without bending constant renormalization ($\alpha = 0$), for $\phi = 1/2$, the structure factor $S(\mathbf{q})$ is finite and positive (i.e., stable) for values of the parameters C and $\pi K(\xi)/T$ inside the shaded region. The various instabilities in $S(\mathbf{q})$ occur at the points (000), (100), (110), and (111) in $\mathbf{q}$-space ; the stability boundaries (where $S(\mathbf{q}_{max}) \to \infty$) are shown as dashed curves. The random mixing estimate of the free energy vanishes along the solid curve ; to the right of this line one expects a global instability to lamellar ordering. Note that all the dependence on ϕ_s is contained in $K(\xi)$.
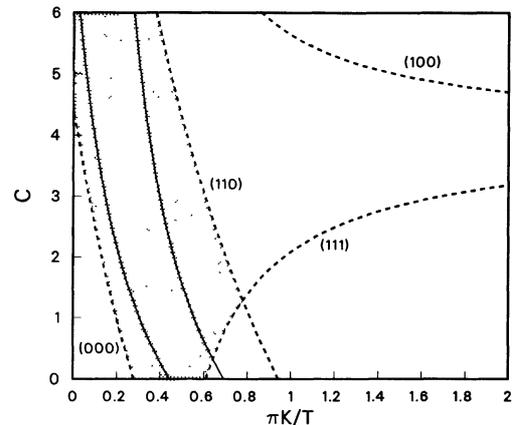

Fig. 5. — The linearly stable region (shaded area) and stability boundaries (dashed curves) for $S(\mathbf{q})$ with bending constant renormalization ($\alpha = 3$, $\phi = 1/2$). The pair of solid curves are the estimated first-order phase boundaries which separate the microemulsion from the lamellar phase (right-hand solid curve) and from coexistence of oil-rich and water-rich phases (left-hand solid curve).

to treat in the context of a lattice model.) Furthermore, since the volume is fixed and the number of lattice sites obeys $N = V/\xi^3$, the number of lattice sites itself depends on the configuration.

For example, if a configuration with $\phi = 1/2$ is ordered in a lamellar fashion, it has only one interface per cell ; if randomly mixed, 3/2 interfaces per cell ; and if ordered with $\mathbf{q} = (110)$ or $\mathbf{q} = (111)$, two or three interfaces per cell respectively.

This means that, at fixed ϕ_s (with $\phi = 1/2$), we have $3/2 \, \xi_{100} = \xi_{rm} = 3/4 \, \xi_{110} = 1/2 \, \xi_{111}$. The lattice spacing in the lamellar-ordered structure must be smaller than in the randomly-mixed state, and the lattice spacings in the two- and three-dimensional antiferromagnetic states are progressively larger than in the randomly mixed state, so that the same amount of surfactant is used per unit volume.

Since our calculation of $S(\mathbf{q})$ counts the bending energy more accurately than a random mixing estimate, one might expect that increasing the bending constant would lead to correlations which would involve a state of fewer bends per cell than the randomly mixed state. Since the system is constrained to contain a fixed amount of surfactant, the natural candidate for these correlations and the eventual divergence in $S(\mathbf{q})$ would be a lamellar instability, $\mathbf{q} = (100)$. Figures 4 and 5 show that this is not the case ; the model predicts a $\mathbf{q} = (110)$ instability as K increases, even though this state has more bends per cell than a randomly mixed state. This paradox requires explanation.

There are two effects which correlations introduce into our model : (i) a change in the bending energy for a correlated systems as opposed to a random one and (ii) a change in the number of cells, and hence in the total free energy. Certainly in equation (13) for $S(\mathbf{q})$ there are terms (the first on the right-hand side) which account for the change in bending energy and configurational entropy per site from a random-mixing estimate, for a system which is ordered in some way. If these were the only terms relevant to $S(\mathbf{q})$, lamellar ordering would indeed be favorable as K was increased.

However, there is another effect of ordering — namely, the change in the number of cells in the system. If the system develops a small amount of lamellar order, the lattice size ξ decreases which implies that the number of cells increases. If we expand about a randomly mixed state, then, one term in the change in free energy per unit volume is estimated by $-3 \, f_{rm}(\xi - \xi_{rm})/\xi_{rm}$. (This is the second term on the right-hand side in Eq. (13).) If the random-mixing free energy is dominated by bending energy and thus positive, decreasing the number of sites tends to make the free energy less positive and more favorable. Hence, a small amount of correlation which increases the lattice size, even though it increases the number of bends per cell, may decrease the free energy per unit volume.

It so happens that for

$$\pi K(\xi)/T > \log (2)/(1 + C/4) \, , \quad \phi = 1/2$$

the free energy of a randomly mixed state is indeed positive ; thus a small fluctuation with wavevector $\mathbf{q} = (110)$ or (111) may actually serve to lower the system free energy. Which wavevector [(110) or (111)] represents the best compromise between

increasing ξ and adding extra bends should and does depend on C, the parameter which weights the cost of a *double bend* (Fig. 2). When C is small, the instability of the model as K is increased appears first in the (111) direction, while for larger C (a high penalty for *double bends*), (110) is the most unstable direction at large K.

Clearly, this paradoxical effect cannot persist as the amplitude of the correlation increases ; the system does not really want all the bends that the perfectly ordered $\mathbf{q} = (110)$ or (111) state contains. Recall, however, that our single-site approximation assumes the fluctuations about random mixing are small. This must break down as K increases and the correlations grow ; the linear stability boundaries of figures 4 and 5 at which the calculated $S(\mathbf{q})$ diverges are thus not physical and cannot be reached. Indeed, we will show below that a first-order transition (global instability) to the lamellar phase intervenes well before the singularity in $S(\mathbf{q})$ is reached ; in the accessible region of parameter space, the correlations predicted by our model are indeed small and our calculation is self-consistent.

3.1.2 *Oil-water phase separation.* — Next we inquire about the nature of the $\mathbf{q} = 0$ singularity which appears in $S(\mathbf{q})$ as K is *decreased*. In models of simple ordering transitions (e.g. Ising models), the random mixing approximation would become better as $K(\xi)/T \to 0$, i.e. in the limit of high temperature. However, for our case where correlations change both the energies and the lattice size, a $\mathbf{q} = 0$ instability — phase separation — is predicted.

This behaviour, which is anomalous for Ising systems but is completely realistic for microemulsions, again results from the variation in the number and size of lattice cells as the configurations become ordered. If the random-mixing estimate of the free energy is dominated by entropy of mixing rather than bending energy, i.e. if $K(\xi)$ is small $[\pi K(\xi)/T < \log (2)/(1 + C/4)$ for $\phi = 1/2]$, the free energy per unit volume can be made more negative by correlations which decrease ξ and increase the number of cells. A $\mathbf{q} = 0$ correlation does precisely this ; as larger regions of pure oil and pure water appear, the surfactant must be taken up by increasingly small *droplets* (single cells) of the opposite phase.

These increasingly numerous droplets have a great deal of configurational entropy ; they also have bending energy of $8\pi K$ per drop, but as $K \to 0$ this becomes negligible. This $\mathbf{q} = 0$ instability, then, remains a plausible description of the physical situation even as the amplitude of the $\mathbf{q} = 0$ correlations becomes large, in contrast to the antiferromagnetic correlations that were found for larger K. We may therefore interpret the $\mathbf{q} = 0$ instability boundary qualitatively as a spinodal line, which represents the

limit of stability of the microemulsion to macroscopic phase separation within our model, and is related to the two- and three-phase equilibria for small ϕ_s shown in figure 1.

3.1.3 First-order phase boundaries.

— In order to better estimate the physical range of parameters for describing microemulsions, we superimpose on our $S(\mathbf{q})$ stability plots, estimates of the first-order phase boundaries between the microemulsion and the lamellar and dilute droplet phases (see Figs. 4, 5). These estimates result from a calculation of the region in K and C where the free energy F of the microemulsion, when plotted as a function of ϕ and ϕ_s, has positive curvature and is negative. At $\phi = 1/2$, the microemulsion is unstable (F has negative curvature) for small values of ϕ_s; this instability corresponds to the phase separations shown in figure 1 and discussed in reference [8]. At large values of the surfactant volume fraction, the random, bicontinuous microemulsion is unstable to an ordered, lamellar phase which to a zeroth order approximation has no entropy of mixing and no bends. We therefore estimate its free energy to be zero, and associate the corresponding phase boundary with the curve $F = 0$ [35].

For the case of no bending constant renormalization (Fig. 4), very little remains of the stable region of $S(\mathbf{q})$, except for unphysically small C (to the left of the solid line in the figure). References [7, 8] assumed $C = 4$ for convenience; $C < 2$ may be interpreted as actually favoring the *double bends* shown in figure 2 over (a pair of) single bends. The absence of a region in which $S(\mathbf{q})$ is linearly stable is consistent with the absence of phase stability for our model without bending constant renormalization ($\alpha = 0$). Previous work [7, 8] found that the microemulsion is only stabilized with respect to the lamellar phase if one introduces a length-dependent bending constant $K(\xi)$ (Eq. (12)). The bending constant must be sufficiently reduced at larger length scales that the nearly random microemulsion may gain configurational entropy over a lamellar phase, without paying too high a price in bending energy.

With bending constant renormalization ($\alpha > 0$), $S(\mathbf{q})$ is found to be stable in a larger and more reasonable region of parameter space (between the solid lines in Fig. 5). Within this region lies a band of parameter values for which the microemulsion is calculated, as described above, to be more stable than the competing lamellar and droplet phases. The various stability and phase boundaries are shown in figure 5 for the case $\alpha = 3$, $\phi = 1/2$.

3.2 $S(\mathbf{q})$ in the accessible region.

— Inside the region of parameter space where the microemulsion is stable, and the value of C is reasonable (e.g., $2 < C < 4$), the correlation function is well-behaved. The maxima of $S(\mathbf{q})$ are small enough [in the range two to four, in units of $S(0)$] for our small-fluctuations assumption to be plausibly self-consistent.

We may now proceed to characterize the correlations present in our calculated $S(\mathbf{q})$. We shall discuss in turn (1) the significance of the direction in q-space of the maximum, and the limitations of the lattice model; (2) the peak position after angular averaging, and the dependence of $S(\mathbf{q})$ on the model parameters C, $K(\xi)$, and ϕ; and (3) the relevance of our calculations to scattering and freeze-fracture experiments.

3.2.1 Lattice effects.

— Our model of the microemulsion, which is based on a cubic lattice and assumes a single length scale, is certainly limited in the variety of configurations it can represent. Nonetheless, we may identify the nature of ordering at a given wavevector by its real-space morphology. We can recognize $\mathbf{q} = (100)$ ordering as lamellar (alternating planes of oil and water cells, with few bends); we interpret (110) ordering as a tendency to form parallel (possibly linked) tubes; and we view (111) correlation as characteristic of an *antiferromagnetic* cubic structure. (See Fig. 3.)

The lattice model also introduces an artifactual Brillouin zone into q-space. Thus, the calculated $S(\mathbf{q})$ can only describe the structure on length scales greater than the cell size ξ. Our lattice model says nothing significant about the experimental scattering intensity $I(q)$ for $q \gg \pi/\xi$. Of course, it is well known that Porod scattering from the interface should dominate at large q, and it may be reasonable for our model to compare experimental $I(q)$ to a powder-average of our $S(\mathbf{q})$ multiplied by some suitably chosen form factor (e.g., polydisperse spheres of mean radius $\approx \xi$). In any case what our model *can* describe are correlations at length scales of the order of a few times ξ, which modify the random mixing description of microemulsions, and which are presumably responsible for the characteristic scattering peak observed experimentally.

3.2.2 Variation of $S(\mathbf{q})$ with C, $K(\xi)$, and ϕ.

— Now consider the dependence of the structure factor on the parameter C within a reasonable range (say, $2 < C < 4$). The structure factor is found to be nearly invariant along curves which are parallel to the estimated phase boundaries. Since the phase boundaries are nearly parallel to the C axis, one need not worry about the precise value of C within this range. (This is fortunate because the model parameter C is not easily related to experiment.)

Next, we scan, across the termodynamically stable region of parameter space, varying $K(\xi)$ and holding C fixed, examining the behaviour of the rotationally averaged structure factor,

$$\bar{S}(q) \equiv \int S(\mathbf{q}) \, d\Omega \, .$$

Figure 6 shows that the peak in $\bar{S}(q)$ quickly moves from q near zero at the left (oil-water phase separation) boundary, to $q \approx \pi/\xi$ for most of the stable region. This shift of the peak occurs because $S(\mathbf{q})$ is large ($O(1)$) at several different wavevectors. Figure 7 displays scans along the (100), (110), and (111) directions of $S(\mathbf{q})$ for a choice of parameters near the middle of the stable region of figure 5. The height of the $q = 0$ peak is greatest very near to the
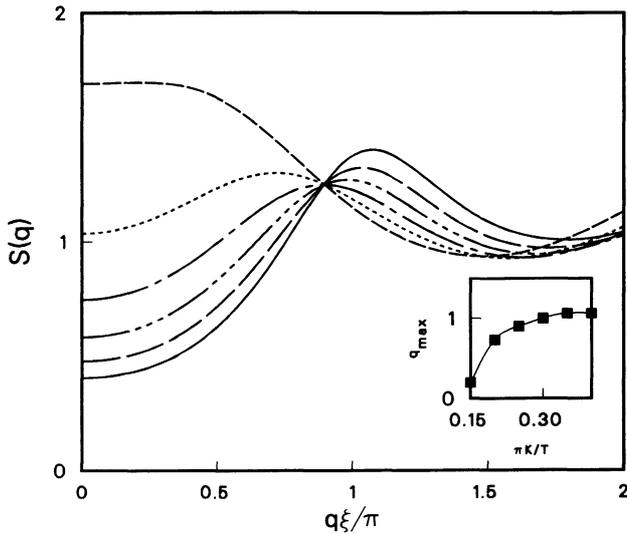

Fig. 6. — The rotationally averaged structure factor, $\bar{S}(q) \equiv \int d\hat{q}\, S(\mathbf{q})$, for $\pi K(\xi)/T = 0.15, 0.20, 0.25, 0.30,$ 0.35, and 0.40. ($\bar{S}(0)$ is a decreasing function of $\pi K/T$, which identifies the curves.) The inset shows the position q_{max} of the peak in $\bar{S}(q)$ as a function of $\pi K(\xi)/T$. These results are for $\phi = 1/2$, $\alpha = 3$, and $C = 3$.
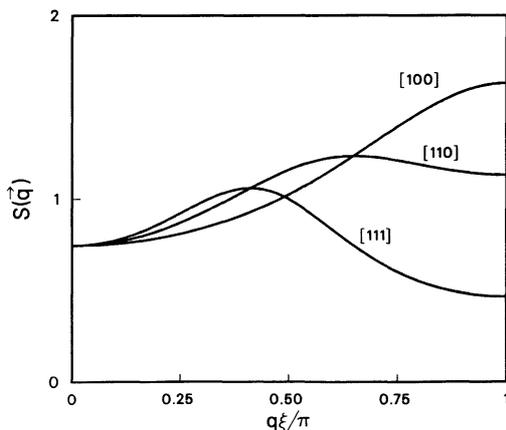

Fig. 7. — The structure factor $S(\mathbf{q})$ along the [100], [110], and [111] directions in q-space. The x-coordinate is the length of each non-zero component of $\mathbf{q}/\pi$ in each scan, i.e. the fraction of the distance from $\mathbf{q} = 0$ to the Brillouin zone boundary. These results are for $\phi = 1/2$, $\alpha = 3$, and $C = 3$.

oil-water separation phase boundary, while the (100) and (110) maxima are somewhat stronger for larger $K(\xi)$.

This variation of $S(\mathbf{q})$ with $K(\xi)$ would seem to indicate a sensitive dependence on the precise value of $K(\xi)$. However, our estimate for the left-hand (oil-water separation) phase boundary as drawn in figure 5 is only a lower bound for the minimum stable $K(\xi)$ at a given C. A more accurate calculation of this phase boundary within the model suggests that it is shifted to larger $K(\xi)$ by as much as one-third of the width of the stable region indicated in figure 5. With this in mind, figure 6 suggests that (for $\phi = 1/2$) the rotationally averaged structure factor is not sensitive to the exact value of $K(\xi)$ in the fully stable region, where $\bar{S}(q)$ may be characterized as having a broad peak near $q = \pi/\xi$ with a ratio $\bar{S}(q_{max})/\bar{S}(0) \approx 2$.

Next, we consider the dependence of $\bar{S}(q)$ on the volume fraction ϕ of water (for typical values of the parameters $K(\xi)$ and C near the middle of the stable region). It turns out that over a wide range ($0.1 < \phi < 0.5$) of volume fractions, the structure factor as a function of the scaled variable $q\xi_{rm}$ undergoes only small changes : $\bar{S}(0)$ rises, and the peak shifts slightly to smaller values of $q\xi$ and diminishes somewhat as ϕ is decreased. (Note that our model, without spontaneous curvature, is symmetric under interchange of ϕ and $1 - \phi$.) This concentration dependence of $\bar{S}(q)$ is in broad agreement with several scattering experiments where the main effect of changing the volume fractions is to change ξ_{rm} as in equation (1). All these results refer to the choice $\alpha = 3$; similar behaviour is seen for other moderately positive values of α.

3.2.3 Real-space structure. — We have constructed real-space lattice configurations with the calculated pairwise correlation function, in order to visualize the effects of the correlations. The configurations are generated by a simulation of the calculated structure factor from an initially random sample of spins of size $20 \times 20 \times 20$. Randomly chosen spin flips are accepted if they reduce the difference between the correlation function of the sample and that calculated for the microemulsion ; the procedure is found to converge readily. This is not in any way a Monte Carlo simulation of the lattice microemulsion, but only a way of visualizing $S(\mathbf{q})$. A typical sample (with $C = ...,$ $\pi K(\xi)/T = ...,$ $\phi = 1/2$) is shown in figure 8 where it is shown alongside an experimental micrograph [24]. Note that an image of this kind contains far more structural information than the angle-averaged $S(\mathbf{q})$, as discussed in section 3.2.1 above.

From such pictures, several observations are evident : (i) the correlations in the stable region are not
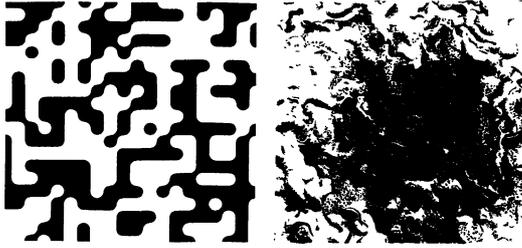
Fig. 8. — A slice of a real-space configuration which has been constructed so that its pairwise correlation function is given by the Fourier transform of $S(q)$. The boundaries between cells of oil (shaded) and water (white) have been smoothed into sections of spheres. The configuration was generated by quenching a random configuration (see section 3.2.3). Freeze fracture electron micrograph of a middle-phase microemulsion (from Ref. [24]). The speckled regions are oil and the smooth regions are water.
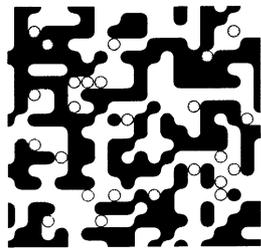

Fig. 9. — The configuration of figure 8 with the changes from random mixing indicated as follows : cells which were initially water-filled but were flipped are shown as darkly cross-hatched ; cells which remained oil-filled are black ; cells which were initially oil-filled but were flipped are shown as lightly cross-hatched circles ; and cells which remained water-filled are white.

very strong (which makes our calculation self-consistent) ; typically, only about 10 per cent of the oil-water spins must flip from the random configuration to converge to the model $S(q)$, as shown in figure 9 ; (ii) the number of *double bends* in the system is reduced by around 10 per cent (for $C \approx 3$) as a result of the correlations, and the lattice size ξ is only very slightly increased (by under one per cent) ; (iii) the generated configurations do not look *lamellar* ; it is not necessary, and is incorrect within the present model, to assume the ordering within a bicontinuous microemulsion, responsible for the peak in $S(q)$, is simply local lamellar ordering ; (iv) finally, it does not seem too fanciful to suggest that the generated pictures stand comparison with real-space images of microemulsions as obtained in freeze-fracture experiments (Fig. 8).

4. Conclusions.

This calculation of the structure factor of a microemulsion is the first such work which is based on a thermodynamic model of microemulsions, and not simply an ad hoc description of the structure. We have found the following results, which were shown to be insensitive to the details and possible lattice artifacts of our coarse-grained model of microemulsions.

(1) The correlations at the scale of a few times the cell size ξ are not strong, which implies that the present calculation based on a small-fluctuation expansion about random mixing is self-consistent. In addition, our previous work which computed the phase diagram of microemulsions assuming a random mixing structure is validated, as the structure is close to random mixing.

(2) The peak in the rotationally-average structure factor $\bar{S}(q)$ is calculated to have a relative height $\bar{S}(q_{max})/\bar{S}(0)$ of about two, within the range of model parameters for which the microemulsion is the phase of lowest free energy. The position q_{max} of the peak is close to π/ξ independent of water volume fraction ϕ, in agreement with experiment. This peak position is simply due to a small amount of order at wavevectors (100) and (110), i.e. to *antiferromagnetic* correlations between neighbouring oil-water spins. The Hamiltonian only contains nearest- and next-nearest neighbour interactions, so this is a natural result.

(3) The structure calculated cannot be viewed as purely local lamellar (100) order, because there is significant strength in $S(q)$ at other wavevectors, in particular (110) ; this would correspond, off lattice, to a locally tubular morphology. It is worth noting anyway that as this calculation includes fluctuations about random mixing to lowest order, no direction for the antiferromagnetic ordering [e.g., (100) as opposed to (010) or (001)] is selected. The absence of strong lamellar correlations is consistent with the experimental observation that the microemulsion/lamellar transition is usually strongly first order in character. Moreover, the real-space structure shown in figure 8, which contains a suitable admixture of weak lamellar (100) and tubular (110) correlations, is qualitatively similar to freeze fracture images of microemulsions while exhibiting a peak in its (angle-averaged) structure factor that remains broadly consistent with observations from scattering experiments.

Acknowledgements.

References

[1] For a general survey see (a) Surfactants in Solution, Eds. K. Mittal, B. Lindman, (Plenum, N.Y.) 1984, and ibid (1987) ;
(b) Physics of Complex and Supermolecular Fluids, Eds. S. A. Safran, N. A. Clark (Wiley, N.Y.) 1987.

[2] CALJE, A., AGEROF, W. G. M., VRIJ, A., in Micellization, Solubilization, and Microemulsions, Ed. K. Mittal (Plenum, N.Y.) 1977, p. 779 ;
OBER, R., TAUPIN, C., J. Phys. Chem. 84 (1980) 2418 ;
CAZABAT, A. M., LANGEVIN, D., J. Chem. Phys. 74 (1981) 3148 ;
ROUX, D., BELLOCQ, A. M., BOTHOREL, P., in reference [1(a)], p. 1843 ;
HUANG, J. S., SAFRAN, S. A., KIM, M. W., GREST, G. S., KOTLARCHYK, M., QUIRKE, N., Phys. Rev. Lett. 53 (1983) 592 ;
KOTLARCHYK, M., CHEN, S. H., HUANG, J. S., KIM, M. W., Phys. Rev. A 29 (1984) 2054.

[3] SCRIVEN, L. E., in Micellization, Solubilization, and Microemulsions, Ed. K. Mittal (Plenum, N.Y.) 1977, p. 877.

[4] DE GENNES, P. G., TAUPIN, C., J. Phys. Chem. 86 (1982) 2294.

[5] HUH, C., J. Colloid Interface Sci. 97 (1984) 201 and 71 (1979) ;
SAFRAN, S. A., TURKEVICH, L. A., Phys. Rev. Lett. 50 (1983) 1930 ;
SAFRAN, S. A., TURKEVICH, L. A., PINCUS, P. A., J. Phys. Lett. France 45 (1984) L69.

[6] WIDOM, B., J. Chem. Phys. 81 (1984) 1030.

[7] SAFRAN, S. A., ROUX, D., CATES, M., ANDELMAN, D., Phys. Rev. Lett. 57 (1986) 491 and in Surfactants in Solution : Modern Aspects, Ed. K. Mittal (Plenum, N.Y.) in press.

[8] ANDELMAN, David, CATES, M., ROUX, D., SAFRAN, S. A., J. Chem. Phys. (in press).

[9] JOUFFROY, J., LEVINSON, P., DE GENNES, P. G., J. Phys. France 43 (1982) 1241.

[10] TALMON, Y., PRAGER, S., J. Chem. Phys. 69 (1978) 2984 and 76 (1982) 1535.

[11] DAVIS, H. T., SCRIVEN, L. E., Soc. Pet. Eng. Repr. #9278, 55th Annual Fall Technical Conf. of the SPE of AIME, Dallas, TX (1980).

[12] WHEELER, J. C., WIDOM, B., J. Am. Chem. Soc. 90 (1968) 3064.

[13] WIDOM, B., J. Chem. Phys. 84 (1986) 6943.

[14] SCHICK, M., SHIH, W. H., Phys. Rev. B 34 (1986) 1797 ;
CHEN, K., EBNER, C., JAYAPRAKASH, C., PANDIT, R., J. Phys. C 20 (1987) L361.

[15] HU, Y., PRAUSNITZ, J. M. (unpublished).

[16] AUVRAY, L., COTTON, J. P., OBER, R., TAUPIN, C., J. Phys. France 45 (1984) 913 and in reference [1(b)] ;

DE GEYER, A., TABONY, J., in Physics of Amphiphilic Layers, Eds. J. Meunier, D. Langevin, N. Boccara (Springer-Verlag, NY) 1987.

[17] KALER, E. W., BENNETT, K. E., DAVIS, H. T., SCRIVEN, L. E., J. Chem. Phys. 79 (1983) 5673 and 5685 ;
CHANG, N. J., KALER, E. W., J. Chem. Phys. (in press).

[18] BERK, N. F., Phys. Rev. Lett. 58 (1987) 2718 ;
TEUBNER, M., STREY, R., J. Chem. Phys. 87 (1987) 3195 ;
TEUBNER, M., (to be published) ;
LICHTERFELD, F., SCHMELING, T., STREY, R., J. Phys. Chem. 90 (1986) 5762.

[19] ZEMB, T. N., HYDE, S. T., DERIAN, P.-J., BARNES, I. S., NINHAM, B. W. (to be published).

[20] ABILLON, O., BINKS, B. P., OTERO, C., LANGEVIN, D., OBER, R. (in press).

[21] EVANS, D. F., MITCHELL, D. J., NINHAM, B., J. Phys. Chem. 90 (1986) 2817 ;
CHEN, J. S., EVANS, D. F., NINHAM, B., J. Phys. Chem. 87 (1983) 538 ;
ANDERSON, D. M., DAVIS, H. T., EVANS, D. F., SCRIVEN, L. E., J. Phys. Chem. (in press).

[22] SAMSETH, J., CHEN, S. H., LITSTER, D., HUANG, J. S. (to be published).

[23] CANDAU, S. J., HIRSCH, E., ZANA, R., J. Colloid Interface Sci. 105 (1985) 521 and in reference [1(b)].

[24] JAHN, W., STREY, R., in Physics of Amphiphilic Layers, Eds. J. Meunier, D. Langevin, N. Boccara (Springer-Verlag, NY) 1987 ;
KALWEIT, M., et al., J. Colloid Interface Sci. 118 (1987) 436.

[25] HELFRICH, W., HARBICH, W., in reference [1(b)] and in Physics of Amphiphilic Layers, Eds. J. Meunier, D. Langevin, N. Boccara (Springer-Verlag, NY) 1987.

[26] VONK, C. G., BILLMAN, J. F., KALER, E. M., J. Chem. Phys. (in press) ;
KALER, E. W., TED DAVID, H., SCRIVEN, L. E., J. Chem. Phys. 79 (1983) 5685 ;
KALER, E. W., PRAGER, S., J. Colloid Interface Sci. 86 (1982) 359.

[27] SAFRAN, S. A., ROUX, D., CATES, M., ANDELMAN, D., in Physics of Amphiphilic Layers, Eds. J. Meunier, D. Langevin, N. Boccara (Springer-Verlag, NY) 1987.

[28] HELFRICH, W., J. Phys. France 46 (1985) 1263 and unpublished.

[29] PELITI, L., LEIBLER, S., Phys. Rev. Lett. 54 (1985) 1690.

[30] FORSTER, D., Phys. Lett. A 114 (1986) 115 ;
KLEINERT, H., Phys. Lett. A 114 (1986) 263.

[31] See, e.g., FEYNMAN, R. P., Statistical Mechanics (Benjamin, NY) 1972.

[32] Terms of order $(1/N)$ are neglected. This results in the fact that the only contributions